Journal of Quantitative Spectroscopy & Radiative Transfer 158 (2015) 84–90

Contents lists available at ScienceDirect

Journal of Quantitative Spectroscopy & Radiative Transfer

journal homepage: www.elsevier.com/locate/jqsrt

Optical properties of thin graphitic nanopetal arrays

Hua Bao [a,*], Anurag Kumar [b], Yuannan Cai [a], Yuzhong Ji [a], Timothy S. Fisher [b], Xiulin Ruan [b,*]

[a] University of Michigan-Shanghai Jiao Tong University Joint Institute, Shanghai Jiao Tong University, Shanghai 200240, China
[b] School of Mechanical Engineering and Birck Nanotechnology Center, Purdue University, West Lafayette, IN 47907, United States

ARTICLE INFO

Article history:
Received 31 August 2014
Received in revised form
5 November 2014
Accepted 24 December 2014
Available online 31 December 2014

Keywords:
Graphite
Thermal radiative property
Petal array

ABSTRACT

Thermal radiative properties of thin graphitic petal arrays are theoretically and experimentally investigated. Finite-difference time-domain (FDTD) simulations are first performed to calculate optical properties of vertical graphitic arrays of different structures, namely, graphitic gratings, periodic graphitic cavities, and random graphitic cavities. For graphitic gratings, the absorptance and reflectance are relatively larger when the incident electric field is parallel to the graphitic plane, while the absorptance and reflectance are both significantly lower when the electric field is polarized perpendicular to the graphitic plane. Ordered graphitic petal cavity arrays show optical properties falling between the above two cases of different polarizations. Random vertical cavity arrays with various angles of orientation show similar properties to ordered petal cavities. For oblique gratings, the reflectance will increase with oblique angle for both polarizations, while the absorptance decreases with oblique angle for the in-plane polarization and increases with oblique angle for the out-of-plane polarization. The oblique effects are explained by the strong anisotropic nature of graphitic petals. The FDTD results are compared to effective medium theory to find that the latter describes the optical properties of the graphitic grating and cavity well, and we propose an approach based on effective medium theory to approximate the dielectric function of graphitic petals with random orientation. The predicted hemispherical total reflectance based on this model gives about 2% reflectance in the visible spectrum and agrees well with experimental data from a fabricated graphitic petals sample.

1. Introduction

Recently optical properties of various nanostructure arrays have received considerable attention for use in a range of potential applications [1–5]. For instance, silicon nanowire arrays demonstrate extremely low reflectance, which is desirable for solar cell applications [3,6]. The low optical reflection in these array structures can be mainly attributed to refractive index matching. Optical resonance in individual nanowires and multiple scattering can also help to trap light very effectively [7–9]. Even with photonic effects in these structures, the absorption in silicon or other semiconductor material is not strong, due to the low intrinsic absorption. In comparison, arrays of aligned multi-walled carbon nanotubes (CNT) exhibit directional emission [10], polarization dependence [11], extremely low reflection [12–14], and relatively high absorption [15,16]. Although it is difficult to build CNT based solar cells, their high intrinsic absorption is important to other engineering applications, such as solar thermal absorbers, radiometric temperature measurements [17], and blackbody sources [18].

* Corresponding authors.
E-mail addresses: hua.bao@sjtu.edu.cn (H. Bao), ruan@purdue.edu (X. Ruan).

http://dx.doi.org/10.1016/j.jqsrt.2014.12.016
0022-4073/

On the other hand, two-dimensional carbon nano-petals can be synthesized under growth conditions similar to those of CNTs [19]. Unlike graphite intercalated compounds such as exfoliated graphene, carbon nano-petals are made without the use of impurity metals, atomically thin, and free-standing. The growth technique and conditions have been discussed in detail elsewhere [20]. The typical thickness of the petals produced using this technique, as estimated from SEM and TEM images, is around 5 nm. Each of these graphite petals grows to a height of order 1 μm. The volume fraction is estimated to be between 8% and 15%, based on the measured mass difference before and after the petal array growth. In more recent experiments it has been observed that selective area growth may be achieved in carbon nano-petal arrays using scratch techniques. Like CNT arrays, these graphitic petals have black color, which implies that they could be an alternative black coating for solar absorption or blackbody source applications. However, the optical properties of such graphitic petal arrays have not been reported yet.

In this study, we perform both theoretical and experimental investigations on optical properties of various vertical graphitic nano-petals. We have calculated the optical properties of graphitic gratings, periodic graphitic cavities, oblique graphitic gratings, and randomly oriented graphitic petals using both FDTD and effective medium theory. Although these structures are idealizations of experimentally synthesized structures, they provide a fundamental understanding of how different collective arrangements can affect the radiative properties of graphitic petals. In addition, we fabricated graphitic petals on highly ordered pyrolytic graphite (HOPG) and have characterized the spectral reflectance. The experimental results are compared with those from theory.

2. Simulation details

Graphitic nano-petals of a few nanometer thickness possess electronic properties similar to that of graphite and thus can be modeled as very thin sheets of graphite. The anisotropic dielectric properties for graphite in the visible regime used in the calculations are taken from Ref. [21]. A few different structures are considered in our simulation, including vertical gratings, periodic cavity, random cavity, and oblique gratings, as shown in Fig. 1. Each graphitic petal has a thickness of 5 nm as typically observed in experiments. The height of graphitic petals in our simulation is 200 nm, which is smaller than the typical height (≈ 1 μm in experiments). It will be shown later that the 200 nm height combined with a perfect-matched layer (PML) can be used to model the top layer of the graphitic structure and obtain the optical absorptance and reflectance spectra of graphitic petals with larger height.

The simulation for each of these cases is set up in a similar manner. The smallest repeating cell is used for gratings, periodic gratings, and oblique gratings. For random cavity, the domain is a square of 200 nm $\times$ 200 nm and the lengths of the petals are randomly chosen a value between 50 and 150 nm. All the simulations have periodic boundary conditions in the xy plane and the z direction is truncated by PML at the top and bottom. The structure sits on the PML layer to model the very top region of the graphitic arrays except the oblique grating case. For the oblique grating, it is difficult to achieve numerical convergence if the structure touches the PML, so we model a suspended grating by leaving a 1000 nm vacuum gap between the bottom of the grating and PML. The volume fraction of each case is kept to be 10%, except for the oblique grating where the volume fraction f increases with the oblique angle θ ($f = 10\%/\cos\theta$).

A virtual Gaussian source is placed 1000 nm above the upper surface of the graphitic petals. Normal incidence is considered for all our simulations. Two power flux monitors are placed above and below the array to measure the transmitted and reflected flux values, which are then normalized by the source power to obtain the transmittance T and reflectance R. For all cases, the reflectance and transmittance are calculated in the wavelength range of 400–1100 nm. The absorptance A is then calculated using the energy conservation $A = 1 - T - R$. The simulations are automatically shut down when the maximum field in the domain decays to 10^{-6} of the maximum electric field of the source. The spatial resolution is 0.5 nm in the x (cross-plane direction), 10 nm in y direction, and 10 nm in the z direction for the vertical gratings. For cavity and random cavity, 0.5 nm, 0.5 nm, and 10 nm are chosen for x, y, and z directions, respectively. For oblique gratings, 0.5 nm resolution is chosen for x and z directions and 10 nm is chosen for the y direction. The mesh sizes for different structures are chosen after careful convergence tests. The above

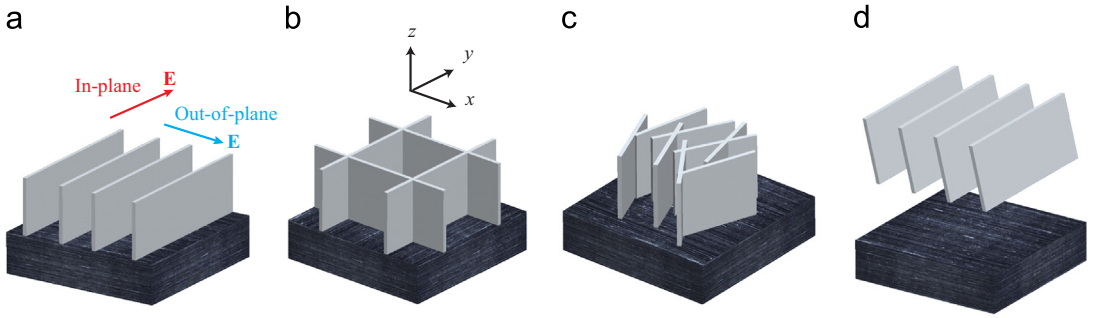

Fig. 1. A sketch of the different graphitic petals we considered: (a) grating, (b) cavity, (c) random cavity, and (d) oblique gratings. For vertical grating and oblique grating, in-plane polarization is defined as the electric field parallel to the graphitic petal and out-of-plane polarization is defined as the electric field perpendicular to the graphitic petal.

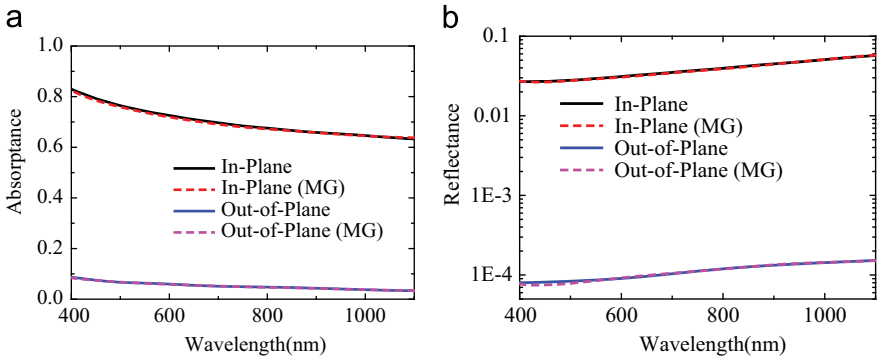

Fig. 2. The absorptance (a) and reflectance (b) of graphitic gratings from FDTD simulations and MG effective medium theory for the graphitic grating structure.

simulations are carried out using the Lumerical FDTD Solutions.

3. Effective medium theory

A less accurate, yet simpler way to obtain optical properties of multi-phase mixture is effective medium theory. Using effective medium theory, one can treat the graphitic petals and air as one homogeneous medium with effective dielectric properties. Effective medium theory generally works well if the feature size is much smaller than the wavelength, as is the case of our graphitic petals. For graphitic petal arrays with relatively small volume fraction (generally 8–15% in experiments), the Maxwell–Garnett (MG) mixing rule can be employed [22]

$$\varepsilon_{i,eff} = \varepsilon_a + \frac{\sum_{j=1}^{n} f_j(\varepsilon_{ij}-\varepsilon_a)\frac{\varepsilon_a}{\varepsilon_a + N_{ij}(\varepsilon_{ij}-\varepsilon_a)}}{1-\sum_{j=1}^{n} f_j(\varepsilon_{ij}-\varepsilon_a)\frac{N_{ij}}{\varepsilon_a + N_{ij}(\varepsilon_{ij}-\varepsilon_a)}} \quad (1)$$

where ε denotes dielectric function, f is volume fraction, N is the depolarization factor, n is the total types of inclusions, subscript i denotes the three directions x, y, z, subscript j denotes the type of mixture, and subscript a means air. For plates, the depolarization factor is 1 in the cross-plane direction and 0 in the in-plane direction. For grating, we can simply obtain the effective dielectric function using Eq. (1) by considering a two phase mixture. Because graphite is anisotropic, the resulted effective medium is also anisotropic. For oblique grating, the diagonalized dielectric tensor along the principal axis (i.e., the in-plane and out-of-plane directions of the petals) is obtained by Eq. (1). This diagonalized dielectric tensor is then rotated by angle θ to obtain the dielectric tensor of the oblique grating. The cavity structure is treated as a mixture of petals with x and y orientations and the air. The effective dielectric function can be obtained by Eq. (1) but considering a three-phase mixture. For completely random orientation structure, we treat it as a four-phase mixture consists of graphitic petals oriented along all three directions and the air. This is a simplification of the random oriented structure, but should preserve the physics. To obtain the optical reflectance and transmittance of the effective medium, we use a similar simulation setup as discussed in Section 2 but with a larger mesh size (10 nm). Even though an analytical formula is available to evaluate the optical property of a homogeneous thin film, it is more convenient to use FDTD to obtain the results. In the subsequent discussions, the results obtained from the effective medium approach are denoted by MG.

4. Results and discussion

4.1. Graphitic gratings

Vertical graphitic petals have been fabricated only recently and little work has been done to achieve good alignment. The petals can in some cases form small domains, or clump-like structures. However, by using scratch techniques, growth of petals with some degree of alignment can be realized. Also, in recent experiment graphene nanoneedles with a certain degree of alignment were observed after anisotropic hydrogen plasma etching of the carbon substrate [23].

The absorptance and reflectance spectra calculated from FDTD simulations and effective medium theory are shown in Fig. 2. Here the term 'in-plane' denotes the electric field parallel to the graphitic petal (magnetic field perpendicular to the petal) and 'out-of-plane' means the electric field perpendicular to the petal, similar to Fig. 1 (d). For the in-plane case we observe high absorptance due to strong optical response in this polarization. The dielectric function that is important here is the component parallel to graphite plane, which has a very high extinction coefficient. The large component of dielectric function in the in-plane direction also gives relatively large reflectance, as shown in Fig. 2(b). When the electric field is perpendicular to the graphitic plane (out-of-plane), the trends are different. The absorptance and reflectance are both lower as compared to the parallel polarization. This is due to the fact that the dielectric function perpendicular to the graphite plane is small, indicating a weak optical response in this polarization. If the height of grating is significantly increased so that the transmission becomes negligible, graphitic gratings can make potentially darker materials than CNTs [15] for the out-of-plane polarized light, due to the extremely low reflectance. In addition, the absorptance and reflectance spectra calculated using MG mixing rule agree very well with FDTD simulations. Due to the relatively small feature size (5 nm thickness)

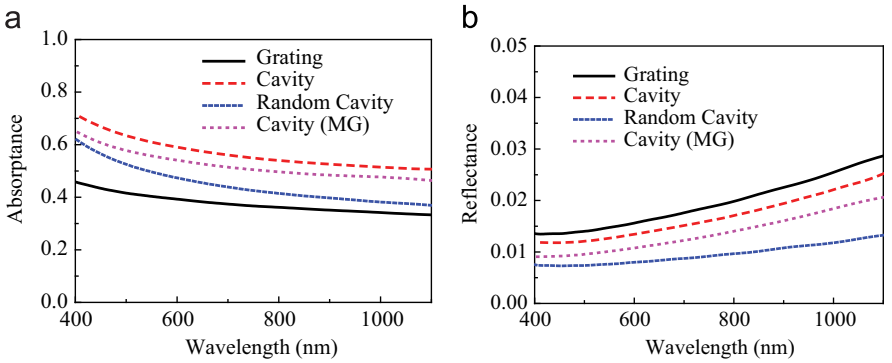

Fig. 3. The absorptance (a) and reflectance (b) of graphitic gratings from FDTD simulations and MG effective medium theory for the graphitic periodic and random cavity structure.

compared to the optical wavelength, it is not surprising that a good agreement can be achieved between effective medium theory and full wave numerical simulation.

4.2. Periodic and random cavity structure

For light absorption applications, it is generally desirable to absorb non-polarized light. Therefore, a cavity structure might be more favorable compared to gratings that is strongly anisotropic. For this structure only a single polarization needs to be considered due to the symmetry. We can expect that the results will be between the two different polarizations for graphitic gratings discussed in the preceding section.

Fig. 3 shows the absorptance and reflectance spectra of periodic and random cavities. For comparison purpose, the absorptance and reflectance of the grating structure (average of both polarizations) and the results from MG effective medium approximation are also shown. It can be observed that a very high absorptance in the range of 50–70% occurs with merely 10% volume fraction and 200 nm height. On the other hand, the reflectance is only less than 3% in the entire visible spectrum. One may note that it is generally difficult to have a material with both low reflectance and high absorption. The unique property of graphitic petals makes it a good candidate for light absorption.

In addition, it could be easier to fabricate vertical petals that have random orientation in the *xy* plane, so we also consider the random oriented structure. The averaged absorptance and reflectance spectra of five different configurations are shown in Fig. 3. Compared with periodic cavity, random cavity has slightly smaller absorptance but also slightly smaller reflectance. This indicates that random orientation in the *xy* plane does not destroy the high absorption and low reflection property of vertical graphitic petals. Comparing the trends shown in Fig. 2 we can see that the reflectance and absorptance for both periodic and random cavity fall between the in-plane and out-of-plane polarizations for graphitic gratings, as expected. However, the absorptance of periodic and random cavity structure are both larger than a simple grating if non-polarized light is considered. The reflectance values for both periodic and random cavity are smaller than a simple grating.

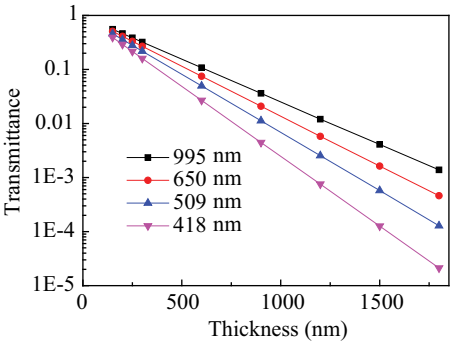

Fig. 4. The total transmittance as a function of height of periodic graphitic petal cavity at different incident wavelengths. Note that the transmittance is shown in log scale, so the transmittance has a clear exponential dependence on the total height of the graphitic petals.

Therefore, the cavity structure is preferred to grating structure for the absorption purpose.

Note that the effective dielectric function obtained by MG mixing rule for periodic cavity and random cavity is the same in our approach, so there is only one MG curve in Fig. 3 (a) and (b). Comparing the MG predictions and FDTD results, the predicted absorptance and reflectance values are similar. There are some discrepancies but should be acceptable for most engineering applications.

4.3. Graphitic petals with larger height

The typical height of the graphitic petals in experiment is about 1 μm depending on the growth time. However, it is practically time consuming to perform a full simulation on such structures. Therefore, as we mentioned above, we use a 200 nm height combined with PML to model the property of the very top 200 nm of the graphitic structure of relatively high petals. To obtain the optical property of petals with larger height, we study how height will change our simulation results for a periodic cavity case. It was found that from 150 to 1800 nm (with PML below), the reflectance values are completely the same (not shown here). The transmitted intensity at the bottom of the cavity structure shows an exponential dependence with thickness as shown in Fig. 4. This indicates that the decay of light intensity in the cavity follows the Beer–Lambert Law,

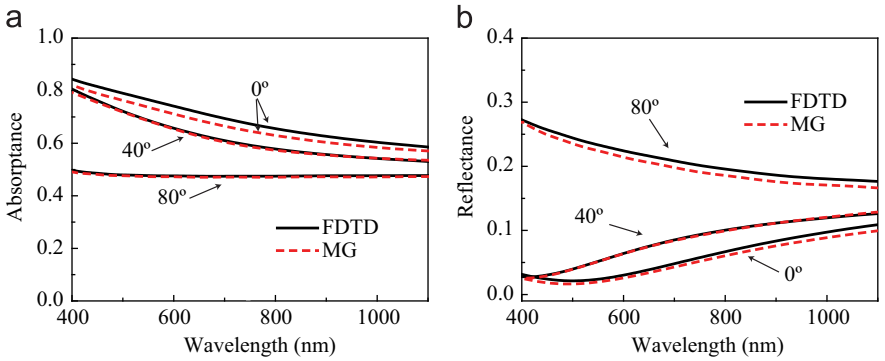

Fig. 5. The absorptance (a) and reflectance (b) of oblique graphitic gratings from FDTD simulations and MG effective medium theory for different angles and in-plane polarization.

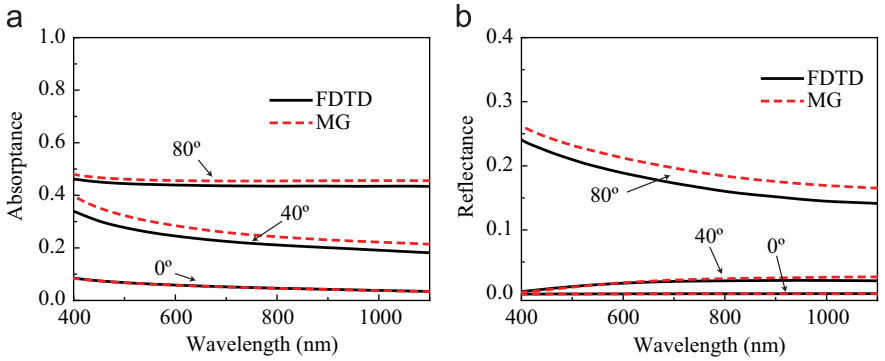

Fig. 6. The absorptance (a) and reflectance (b) of oblique graphitic gratings from FDTD simulations and MG effective medium theory for different angles and out-of-plane polarization.

the same as a typical bulk material. Therefore, the intensity of light in the graphitic cavity for a wavelength λ follows

$$I_\lambda(z) = I_{T0,\lambda} \exp(-\alpha_\lambda z) \tag{2}$$

where I_λ is the reflected intensity, I_{T0} is the transmitted intensity at the air/petal interface, z is the depth from the interface, and α is absorption coefficient of material. Therefore, the general absorption coefficient α for a relatively thick graphitic cavity can be calculated using the results for the 200 nm thickness based on the following equation:

$$A_\lambda(z) = (1-R_\lambda)\cdot[1-\exp(-\alpha_\lambda z)]. \tag{3}$$

where A_λ and R_λ are the spectral absorptance and reflectance, respectively. Without further justification, we expect that the reflectance and absorptance presented in Figs. 2 and 3 for gratings and random cavity can also be used to obtain the reflectance and absorption coefficient of relatively higher grating and random cavity structures.

4.4. Oblique grating

Graphitic petals fabricated in experiment usually contain oblique petals. Previous investigations on carbon nanotube structures show that obliqueness may have a strong effect on the optical properties [16]. In order to capture this effect, we should ideally consider random oblique petals. However, due to the difficulty of numerical simulation for random oblique structures, we first consider aligned oblique grating to see how incline angle can alter the optical property of these petals. Again due to numerical difficulty, oblique grating suspended in air is modeled (unlike other cases that have PML below). The vertical gratings have a height of 200 nm and for oblique ones the projected height in z direction is $200\cdot\cos\theta$ nm where θ is the oblique angle.

Similar to the vertical grating structures, we need to consider two different polarizations as indicated in Fig. 1(d). The absorptance and reflectance for the 0° (vertical), 40°, and 80° gratings and in-plane polarization are shown in Fig. 5. We can see that as the oblique angle increases, the absorptance becomes smaller and the reflectance becomes larger. This is a combined result of larger volume fraction and smaller height when the oblique angle is larger. The results for out-of-plane polarization is shown in Fig. 6. Different from the in-plane case, both absorptance and reflectance increase as the oblique angle increases. The out-of-plane polarization is different from in-plane case because when the gratings become oblique, the electric field is no longer perpendicular to the plane of graphitic petals. In that case, the in-plane dielectric function of graphite starts to play a role. Graphite has a stronger response to electric field perpendicular to the graphitic planes, so that it will have both stronger absorption and reflection, as is shown in Fig. 6. In addition, we

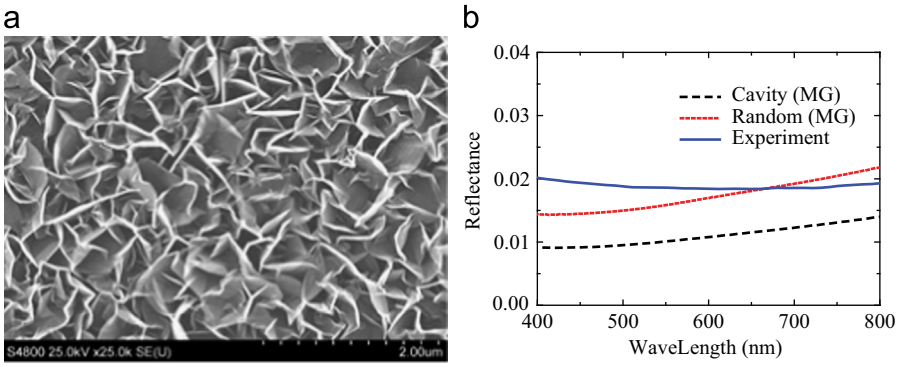

Fig. 7. (a) SEM images of aligned graphitic petals on HOPG substrate. (b) Calculated reflectance of random cavity and random oriented petals from MG effective medium approximation and the experimental reflectance.

find that the predictions from MG also agree well with full wave FDTD simulations for oblique graphitic gratings.

4.5. Comparison with experiment

To provide an experimental comparison and justify our simulation results, we have synthesized thin graphitic petal arrays in a SEKI AX5200S microwave plasma chemical vapor deposition (MPCVD) system with H_2 (50 sccm) and CH_4 (10 sccm) as the primary feed gases. The substrate was placed in the chamber on a Mo puck and was kept at a height of 15 mm from the puck surface by ceramic spacers. The elevation of the substrate above Mo puck was found to be critical for the growth of the arrays. The elevation ensures a strong coupling between the plasma and the growth substrate. The MPCVD chamber was evacuated to a base pressure of 2 Torr and then filled with high-purity hydrogen at a pressure of 10 Torr. CH_4 was introduced into the chamber, after igniting the hydrogen plasma at 500 W or 700 W with a chamber pressure of 20 Torr to 30 Torr for a period of 15 min. Higher plasma power (700 W) at higher pressure (30 Torr) leads to dense growth over the entire substrate, whereas lower plasma power (500 W) at lower pressure (20 Torr) results in less dense growth, including partial coverage of the substrate surface in some regions. Growth of petals does not require any supplemental heating. The growth substrate couples strongly with the plasma and which is sufficient to locally heat the substrate up to about 1000 °C [24,25,19,26]. Fig. 7(a) shows an SEM image of a region with dense petal growth at 500 W at 20 Torr for 15 min growth duration.

As the sample is grown on an opaque substrate, only the reflectance can be measured. The total hemispherical reflectance was measured using a PerkinElmer Lambda 950 spectrometer with a 150 mm spectralon-coated integrating sphere. Because the samples have low reflectance, the reference beam is attenuated to 1% of the sample beam to ensure accuracy. The measured relative reflectance is normalized by the standard reflectance of spectralon to obtain the reflectance of the graphitic petals. The measured reflectance is around 2% over the entire visible range, as shown in Fig. 7(b).

One may notice that from Fig. 7(a) that the graphitic petals are not as well aligned as modeled above. In order to make a fair comparison with experiment, it is necessary to consider random orientation of graphitic petals. Such a system is very difficult to simulate using FDTD simulations, so we choose to use MG effective medium approximation, which has been shown in preceding sections to generally reproduce the FDTD results. For the random orientation, we consider a four-phase dielectric mixture, including air and the graphitic petals oriented along the three directions. This is obvious a simplification of the problem since the completely random structure may have other effects such as multiple scattering. Yet it should still give reasonable results, considering that MG results agree very well with FDTD in all the vertically aligned cases. Here we simulate an effective medium with 10% volume fraction and 1 μm thickness on a graphite substrate to be comparable with experiment, and the results are shown in Fig. 7 (b). The optical reflectance of vertical petals with same volume fraction and thickness is also shown in the same figure for comparison. It can be seen that reflectance for random orientation is also around 2% in the visible spectrum. Although the wavelength dependence is slightly different, the agreement in the reflectance values is remarkable considering all the simplifications we have made to obtain this results. This agreement in turn justifies our simplification and effective medium approach. In comparison, the vertical petal case shows smaller reflectance because the inclined petals are not considered. Those oblique petals have a relatively important contribution to the reflectance, based on the foregoing results on oblique gratings.

5. Summary

In summary, we investigated the optical properties of graphitic petals in different arrangement, including vertical gratings, cavity, random cavity, and oblique gratings, using the FDTD method and effective medium approximation. It is found that vertical gratings with 10% volume fraction can achieve extremely small reflection (on the order of 10^{-4}) for out-of-plane polarization. For in-plane polarization the optical reflectance is larger and absorption is stronger. For unpolarized light, periodic cavity structure can achieve smaller reflection and larger absorption than simple grating structure. Random cavity has similar property to periodic cavity but with slightly smaller reflection

and absorption. If the petals are oblique, the in-plane dielectric function starts to play an important role so that the overall reflection will increase as the oblique angle becomes larger. For all these cases, we find that effective medium approximation can achieve a good agreement with FDTD simulations. We also fabricated graphitic petals and measure its reflectance, which is around 2% in the entire visible spectrum. We propose an effective medium approach to model the dielectric property of random oriented petals as observed in our experiment. The calculated reflectance based on this model can achieve quantitative agreement with experimental results.

Acknowledgments

This work is partly supported by the Air Force Office of Scientific Research through the Discovery Challenge Thrust (DCT) Program (Grant no. FA9550-08-1-0126, Program Manager Joan Fuller). This work is also partly supported by the National Natural Science Foundation of China (No. 51306111) and Shanghai Municipal Natural Science Foundation (No. 13ZR1456000). Fruitful discussions with Professor Zhuomin Zhang at the Georgia Institute of Technology are gratefully appreciated. H.B. would like to thank Han Xie for the assistance to plot some figures.

References

[1] Tian B, Zheng X, Kempa TJ, Fang Y, Yu N, Yu G, et al. Nature 2007;229:885.
[2] Cao LY, Fan PY, Vasudev AP, White JS, Yu Z, Cai W, et al. Nano Lett 2010;10:439.
[3] Tsakalakos L, Balch J, Fronheiser J, Korevaar BA, Sulima O, Rand J. Appl Phys Lett 2007;91:233117.
[4] Wang XJ, Flicker JD, Lee BJ, Ready WJ, Zhang ZM. Nanotechnology 2009;20:215704.
[5] Diedenhofen SL, Vecchi G, Algra RE, Hartsuiker A, Muskens OL, Immink G, et al. Adv Mater 2009;21:1.
[6] Hu L, Chen G. Nano Lett 2007;7:3249.
[7] Bao H, Ruan XL. Opt Lett 2010;35:3378.
[8] Cao LY, White JS, Park JS, Schuller JA, Clemens BM, Brongersma ML. Nat Mater 2009;8:643.
[9] Muskens OL, Rivas JG, Algra RE, Bakkers EPAA, Lagendijk A. Nano Lett 2008;8:2638.
[10] Wang Y, Kempa K, Kimball B, Carlson JB, Benham G, Li WZ, et al. Appl Phys Lett 2004;85:2607.
[11] Wasik M, Judek J, Zdrojek M. Carbon 2013;64:550.
[12] Yang Z-P, Ci L, Bur JA, Lin S-Y, Ajayan PM. Nano Lett 2008;8:446.
[13] Mizuno K, Ishii J, Kishida H, Hayamizu Y, Yasuda S, Futaba DN, et al. Proc Natl Acad Sci 2009;106:6044.
[14] Tomlin N, Curtin A, White M, Lehman J. Carbon 2014;74:329.
[15] Bao H, Ruan XL, Fisher TS. Opt Express 2010;18:6347.
[16] Bao H, Duvvuri B, Lou M, Ruan X. J Quant Spectrosc Radiat Transf 2014;132:22.
[17] Zhang ZM, Tsai BK, Machin G. Radiometric temperature measurements: I&II. New York: Academic; 2010.
[18] Fainchtein R, Brown DM, Siegrist KM, Monica AH, Hwang E, Milner SD, et al. Phys Rev B 2012;85:125432.
[19] Bhuvana T, Kumar A, Sood A, Gerzeski RH, Hu J, Bhadram VS, et al. ACS Appl Mater Interfaces 2010;2:644.
[20] Zhu M, Wang J, Holloway BC, Outlaw RA, Zhao X, Hou K, et al. Carbon 2007;45:2229.
[21] Johnson LG, Dresselhaus G. Phys Rev B 1973;7:2275.
[22] Wang H, Liu XL, Wang LP, Zhang ZM. Int J Thermal Sci 2013;65:62.
[23] Matsumoto T, Koizumi T, Kawakami Y, Okamoto K, Tomita M. Opt Express 2013;21:30964.
[24] Xiong G, Hembram K, Zakharov DN, Reifenberger RG, Fisher TS. Diam Relat Mater 2012;27:1.
[25] Rout CS, Kumar A, Kumar N, Sundaresan A, Fisher TS. Nanoscale 2011;3:900.
[26] Kumar A, Voevodin AA, Zemlyanov D, Zakharov DN, Fisher TS. Carbon 2012;50:1546.